Plasmonics for advance single-molecule fluorescence spectroscopy and imaging in biology

Cecilia Zaza[1] and Sabrina Simoncelli[1,2]*

[1]London Centre for Nanotechnology, University College London, London, United Kingdom,
[2]Department of Chemistry, University College London, London, United Kingdom

The elucidation of complex biological processes often requires monitoring the dynamics and spatial organization of multiple distinct proteins organized on the sub-micron scale. This length scale is well below the diffraction limit of light, and as such not accessible by classical optical techniques. Further, the high molecular concentrations found in living cells, typically in the micro- to mili-molar range, preclude single-molecule detection in confocal volumes, essential to quantify affinity constants and protein-protein reaction rates in their physiological environment. To push the boundaries of the current state of the art in single-molecule fluorescence imaging and spectroscopy, plasmonic materials offer encouraging perspectives. From thin metallic films to complex nano-antenna structures, the near-field electromagnetic coupling between the electronic transitions of single emitters and plasmon resonances can be exploited to expand the toolbox of single-molecule based fluorescence imaging and spectroscopy approaches. Here, we review two of the most current and promising approaches to study biological processes with unattainable level of detail. On one side, we discuss how the reduction of the fluorescence lifetime of a molecule as it approaches a thin metallic film can be exploited to decode axial information with nanoscale precision. On the other, we review how the tremendous progress on the design of plasmonic antennas that can amplify and confine optical fields at the nanoscale, powered a revolution in fluorescence correlation spectroscopy. Besides method development, we also focus in describing the most interesting biological application of both technologies.

KEYWORDS

plasmonics, nano-antennas, single-molecule fluorescence correlation spectroscopy, single-molecule fluorescence imaging, near-field coupling, biological applications

1 Introduction

Exciting opportunities exist for combining plasmonics with microscopy and spectroscopy techniques (Simoncelli et al., 2016; Simoncelli et al., 2018). Some of the simplest synergic combinations of the two started with thin metallic films (Vasilev et al., 2004), quickly evolving to nanostructured metallic materials than can provide strong

confinement of electromagnetic field intensity by coupling light with localized surface plasmon resonances (Purcell et al., 1946; Anger et al., 2006; Sultangaziyev and Bukasov, 2020). These fields can interact with fluorophores increasing excitation rate, raising quantum yield, and giving control of the far field angular distribution of the fluorescent emitted light (Ford and Weber, 1984). This effect occurs at characteristic distances (Enderlein, 1999). At short distances from the metal surface, strong quenching of radiative transitions occurs due to energy transfer between a fluorophore and a metal (Anger et al., 2006). At longer distances, below the decay length of surface plasmon field, the surface plasmons emissions becomes dominant providing a pathway to increase the intrinsic fluorescence of molecules located in their vicinity. Over decades, this phenomenon has been used for a wide variety of applications in biosensors and imaging (Bauch et al., 2014). However, to date, only a handful of plasmonic-based approaches have been able to push the boundaries of the current state-of-the-art in fluorescence microscopy and spectroscopy. These include techniques such as localized plasmonic structured illumination microscopy (LPSIM) (Bezryadina et al., 2018); plasmon-assisted stimulated emission depletion (STED) nanoscopy (Cortés et al., 2016); surface-enhanced Raman spectroscopy combined with stochastic optical reconstruction microscopy (SERS-STORM) (Olson et al., 2016), among others. Although useful these approaches have yet not been expanded to investigate open questions in the field of biology.
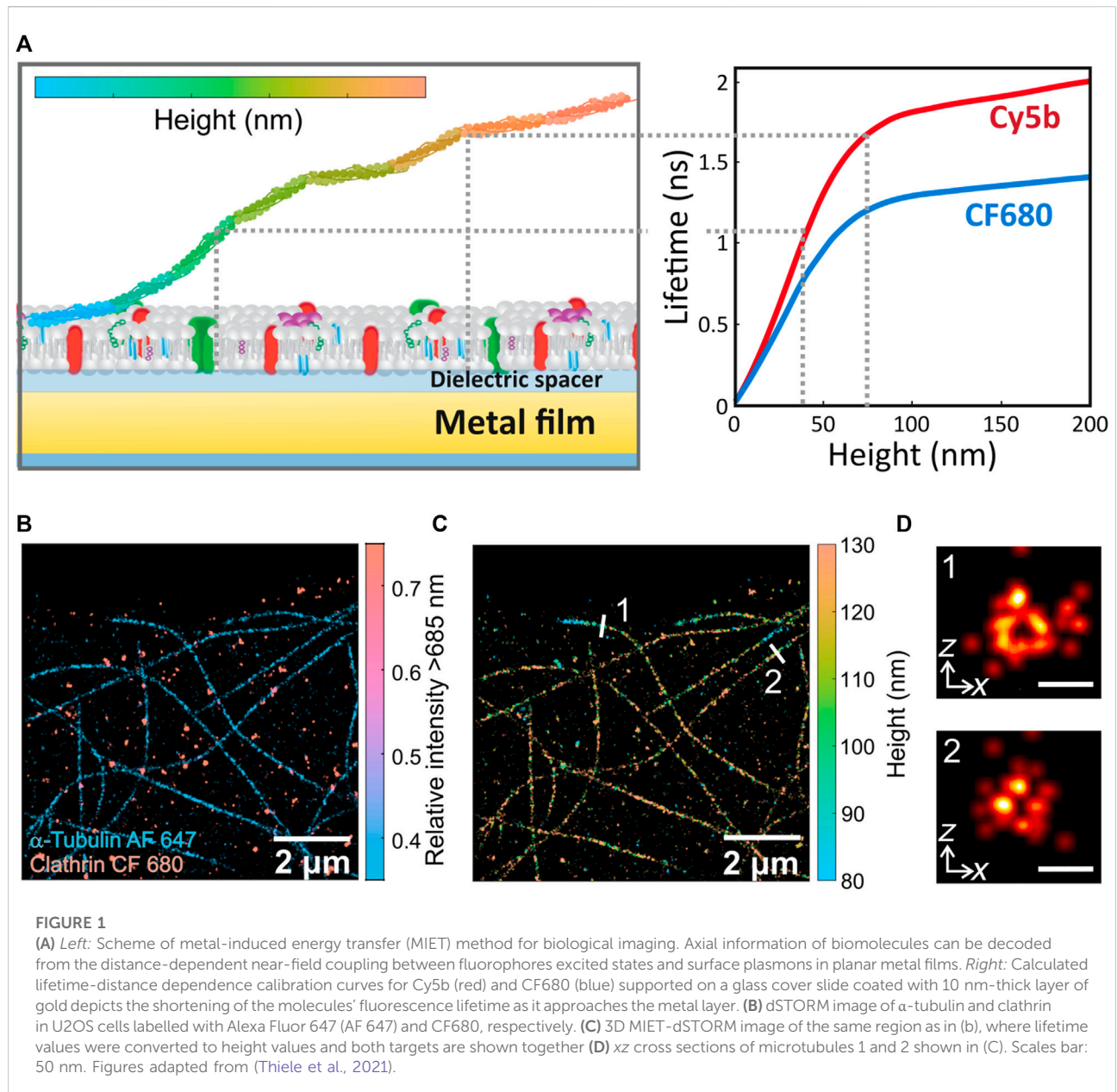
In this review, we mainly focus on the most novel applications, that take advantage of the near-field coupling between single emitters and surface plasmon modes, to develop nano-imaging and nano-spectroscopy technologies with demonstrated capability of exploring biological process with nanoscale spatial- and microsecond temporal-resolution. First, we describe the development of metal-induced energy transfer (MIET), a method capable of exploiting the distance-dependent fluorophore-metal interaction to achieve sub-diffraction axial resolution when combined with fluorescence lifetime imaging microscopy (Chizhik et al., 2014; Simoncelli et al., 2017). Since its inception, MIET has matured not only in terms of technological development, but also in the breadth of applications in the field of biology. This year, it has reached a milestone by allowing researchers to achieve isotropic three-dimensional super-resolution imaging of subcellular structures when combined with single-molecule based super-resolution microscopy (Thiele et al., 2022). Secondly, we review recent breakthroughs in plasmonic antennas arrays that allow to visualize single-molecule dynamics at high concentration ranges, providing a major leap forward in fluorescence correlation and cross-correlation spectroscopy (FCS/FCCS) techniques (Punj et al., 2013a). The tight light confinement of localized plasmonic fields tuned by proper antenna design make them powerful tools to reduce the focusing volume in FCS, thus

increasing the working concentration of fluorophores to relevant physiological conditions, *i.e.*, from nano- to the milli-molar level. In the context of biology, thanks to the higher level of spatial resolution provided by plasmonic antenna FCS, it was recently possible to shed light on the temporal dynamics and size of lipid nano-domains in cell membranes, thus reconciling contrasting views in the scientific community (Winkler et al., 2017). Finally, we provide possible perspectives for new combinations of plasmonics with single-molecule imaging and spectroscopy techniques.

2 Plasmonic substrates for axial nanometer cell imaging

MIET decodes the absolute position of fluorescent molecules located in the vicinity of a thin metallic layer by leveraging the distance-dependent fluorescence lifetime modulation (Chizhik et al., 2014). The fluorescence lifetime is the period of time a fluorophore spends in the excited state before emitting a photon and returning to the ground state (Lakowicz, 2006). The decay rates of a fluorophore are modified by proximity to a metal surface, which affects the fluorophore's lifetime, as happens in Förster resonance energy transfer (FRET) (Lukosz and Kunz, 1977; Chance et al., 1978). Namely, the photons' return to the ground state accelerates as the fluorescent emitter gets closer to a metallic surface, typically gold, resulting in a shorter lifetime (Chizhik et al., 2011; Chizhik et al., 2012; Chizhik et al., 2013). This is proportional to the distance from the gold surface (that acts as an acceptor) and, in contrast to FRET, has a large dynamic range up to around 200 nm above the surface plane (Figure 1A). The modulation of the fluorescence lifetime signal, however, is not only dependent on the fluorophore-surface distance, but also on the material and thickness of the metal layer, the overlap between the plasmon surface resonance and the fluorophore's absorption and emission bands, as well as the fluorophore's emission quantum yield (Gregor et al., 2019). To transform lifetime information into axial distances, the emitter distance-lifetime dependence can be calculated by modelling the emission properties of an emitter above a metallic surface (Chizhik et al., 2014). Figure 1A shows some example calculations for the lifetime-distance dependent signal of Cy5b and CF680 dye supported on 10 nm-thick layer of gold (Thiele et al., 2021), where the monotonous relation between lifetime and axial distance is observed up to around 75 nm. To ease the implementation of MIET, the group of Enderlein has developed a MATLAB-based graphical user interface that automatize the conversion of lifetime to height information with user-defined experimental parameters (Chizhik and Enderlein, 2020).

Berndt and colleagues were the first to take advantage of the strong distance dependence of this energy transfer process to infer axial distances from fluorescence lifetime experiments in a

FIGURE 1
(A) *Left:* Scheme of metal-induced energy transfer (MIET) method for biological imaging. Axial information of biomolecules can be decoded from the distance-dependent near-field coupling between fluorophores excited states and surface plasmons in planar metal films. *Right:* Calculated lifetime-distance dependence calibration curves for Cy5b (red) and CF680 (blue) supported on a glass cover slide coated with 10 nm-thick layer of gold depicts the shortening of the molecules' fluorescence lifetime as it approaches the metal layer. **(B)** dSTORM image of α-tubulin and clathrin in U2OS cells labelled with Alexa Fluor 647 (AF 647) and CF680, respectively. **(C)** 3D MIET-dSTORM image of the same region as in (b), where lifetime values were converted to height values and both targets are shown together **(D)** *xz* cross sections of microtubules 1 and 2 shown in (C). Scales bar: 50 nm. Figures adapted from (Thiele et al., 2021).

biological system (Berndt et al., 2010). Specifically, they imaged microtubules attached to a gold surface via different molecular spacers: avidin, neutravidin and kinesin-1. By measuring the lifetime in a wide-field time-domain fluorescence lifetime imaging microscope, they were able to obtain the molecular dimensions, in the axial axis, of the microtubule-attached proteins with nanometer precision. A couple of years later, Chizhik and colleagues also used this technique to measure the basal membrane of living MDA-MB-231 cells, but in this case with a confocal microscope capable of performing time correlated single photon counting (TCSPC) to quantify lifetime

in each pixel (Chizhik et al., 2014). They measured cell-substrate distances between 50 and 100 nm for various cell types and found differences in cell-substrate distances between three cell lines (MDA-MB-231, A549 and MDCK-II). Cade and colleagues showed this technique using a nanostructured silver film, obtaining height maps of carcinoma cells. They claim that silver films provide better axial sensitivity than gold because radiative decay processes dominate, even when close to the metal, resulting in higher signal levels from fluorophores close to the substrate (Cade et al., 2015). Also, MIET has been used in combination with other techniques such as atomic force

microscopy (Port et al., 2022). In this work, Port and colleagues applied a force with the cantilever forming a new focal adhesion on living cells and at the same time they measured the height of the actin skeleton of NIH 3T3 mouse fibroblasts detecting alterations in the units connecting the actin cytoskeleton to the extracellular matrix (Gottschalk et al., 2022). They also studied the influence of shape induced tension on the height of the actin cytoskeleton (Grandy et al., 2022).

A couple of years later, Chizhik and colleagues measured the axial distance between two proteins in the inner and outer part of the nuclear membrane (Chizhik et al., 2017). Performing dual-color MIET to spectrally separate the signals of the two antibody-labelled proteins, they could determine the distance between those two proteins with nanometric resolution, obtaining a thickness of the nuclear envelope of 30–35 nm which is comparable to electron microscopy measurements. Also, the temporal spreading and adhesion of living platelet to surfaces were investigated via MIET using a confocal microscope with fast scan (Zelená et al., 2020). Hwang and colleagues used MIET to prove a nanometer sectioning method in a large field-of-view in a confocal microscope with a low numerical aperture objective. They tested the method in human aortic endothelial imaging a large field-of-view of 120 μm × 96 μm (Hwang et al., 2021).
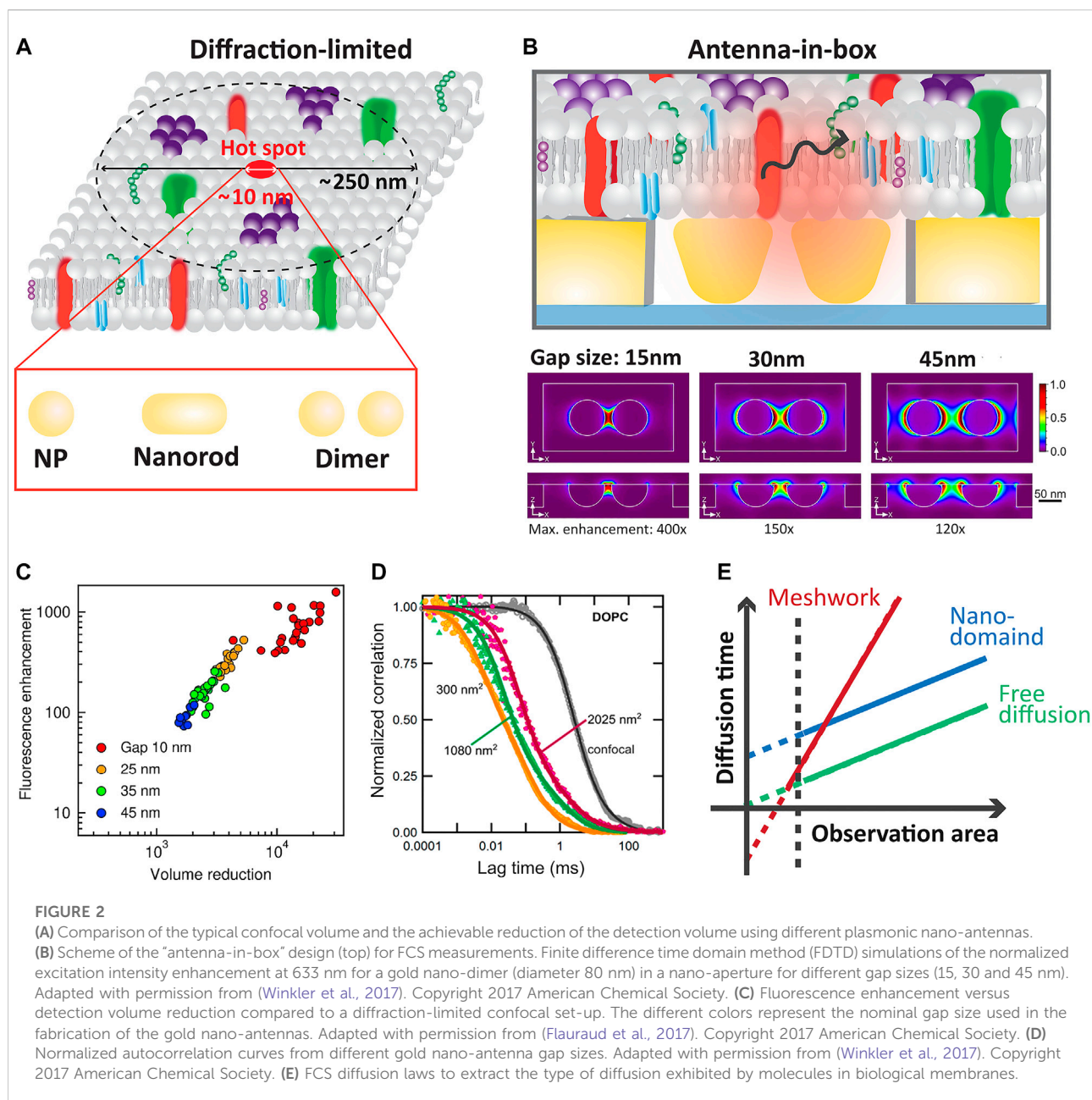
Up to this point, the information obtained was diffraction limited in the lateral dimension. As a result, a combination of MIET and FRET was developed to obtain additional nanometric information in the imaging plane (Chizhik et al., 2018). Axial distances of actin and vinculin were used to elucidate the 3D structure of focal adhesions in hMSCs cells at different points of seeding and the lateral distance between both proteins was inferred via FRET. Karedla and colleagues were the first to combine MIET with single-molecule detection (smMIET), first by measuring the axial distance of single molecules located at different distances (20–50 nm) from a gold film using SiO_2 spacers (Karedla et al., 2014; Karedla et al., 2018) and then by determining axial distances on a DNA origami platform (Isbaner et al., 2018). These works represented the steppingstones to apply MIET in the field of super-resolution fluorescence microscopy, particularly single-molecule localization microscopy (SMLM).

The basic concept of SMLM lies on separating the emission of fluorophores temporally and spatially to pinpoint with a precision much higher than the size of the signal itself the position of each emitter. The lateral localization accuracy in SMLM depends on the number of emitted photons. Therefore, using fluorophores with high absorption cross section and emission quantum yield it is possible to reconstruct super-resolved images with sub-20 nm resolution in xy (Masullo et al., 2021). For example, with ATTO655 that has a quantum yield of 30% and using an SMLM known as DNA point accumulation for imaging in nanoscale topography (DNA-PAINT) a spatial resolution of 6 nm could be achieved (Raab et al., 2014). Axial resolution in SMLM, on the other hand, is typically two- to four-fold worst depending on the methodology

(Huang et al., 2008). Therefore, the possibility to combine MIET with SMLM offers a direct avenue to achieve nanometric isotropic resolution in 3D in a simple fashion. In 2020, with the invention of the new wide-field TCSPC cameras, Oleksiievets and colleagues perform single-molecule FLIM of three fluorophores with similar emission spectra and they could distinguish them with lifetime (Oleksiievets et al., 2020). Super-resolution imaging could not be achieved at this point because of the low quantum yield of this camera, which has rapidly improved over the past two years. At about the same time, Thiele and colleagues developed a method to perform SMLM in a time resolved confocal microscope and used it to perform multiplexed measurements (Thiele et al., 2020; Oleksiievets et al., 2022a). First, they validated their technique by imaging, via two different SMLM modalities: dSTORM and DNA-PAINT, β-tubulin and clathrin in COS-7 cells, labelled with ATTO647 and ATTO655, respectively. These experiments demonstrated that their optical configuration was suitable to perform SMLM experiments whilst decoding color information via the emitter's fluorescence lifetime. They also performed single-molecule measurements in different spectral regions with the two experimental approaches: confocal or widefield and compared both performances in 3D localization of single emitters with MIET (Oleksiievets et al., 2022b). Finally, in 2022, Thiele and colleagues demonstrated, for the first time, isotropic 3D super-resolution imaging using the combination of dSTORM and MIET [17] as schematically illustrated in Figure 1A (Thiele et al., 2021). Specifically, single molecules are localized in each of the confocal binned frames. Then, each single-molecule burst is assigned a lifetime, which is finally transformed into an axial position using the calibration curve that relates lifetime to height. They could obtain images of microtubules and perform multiplexed measurements with the addition of a dichroic mirror. Figure 1B shows a super-resolved image of α-tubulin and clathrin in U2OS cells labelled with Alexa Fluor 647 and CF 680, respectively, where each fluorophore type is represented by a different color. Each channel's lifetime information provides axial distances for both dyes. Figure 1C shows the same microtubules image as Figure 1B, where color represents axial distances in a 3D super-resolved image. With this configuration, the authors were able to resolve the xz profile of the hollow interior of microtubules (~35 nm in diameter), as shown in Figure 1D, highlighting the superior axial resolution of their technique in comparison to the most conventional astigmatic imaging.

3 Plasmonic nano-antennas for live cell fluorescence spectroscopy

Fluorescence correlation spectroscopy (FCS) is a technique that provide dynamic information with high temporal resolution (Krichevsky and Bonnet, 2002a). FCS records the temporal

FIGURE 2
(A) Comparison of the typical confocal volume and the achievable reduction of the detection volume using different plasmonic nano-antennas.
(B) Scheme of the "antenna-in-box" design (top) for FCS measurements. Finite difference time domain method (FDTD) simulations of the normalized excitation intensity enhancement at 633 nm for a gold nano-dimer (diameter 80 nm) in a nano-aperture for different gap sizes (15, 30 and 45 nm). Adapted with permission from (Winkler et al., 2017). Copyright 2017 American Chemical Society. **(C)** Fluorescence enhancement versus detection volume reduction compared to a diffraction-limited confocal set-up. The different colors represent the nominal gap size used in the fabrication of the gold nano-antennas. Adapted with permission from (Flauraud et al., 2017). Copyright 2017 American Chemical Society. **(D)** Normalized autocorrelation curves from different gold nano-antenna gap sizes. Adapted with permission from (Winkler et al., 2017). Copyright 2017 American Chemical Society. **(E)** FCS diffusion laws to extract the type of diffusion exhibited by molecules in biological membranes.

fluctuations caused by fluorescently tag single molecules as they transient through a small observation volume. Since its inception (Magde et al., 1972), FCS has been used to study chemical and biological process by giving access to molecular concentration and molecular diffusion constants (Krichevsky and Bonnet, 2002b). Even further, dual-color cross-correlation fluorescence spectroscopy (FCCS) allows quantification of interacting molecules by providing access to affinity constants and reaction rates (Krieger et al., 2014). However, most FCS modalities use a diffraction limited single focal spot for the measurements. This not only limits the statistical power of the

technique, but it also precludes single-molecule detection in the relevant physiological concentration ranges where most biological reaction occurs. To go beyond the current state of the art of FCS technologies, plasmonic nano-antennas have been used to enable single-molecule sensitivity at micromolar concentration ranges (Figure 2A). The fluorescent signal of molecules diffusing nearby plasmonic antennas can be modified through resonant coupling of the electronic transitions of both parties (Simoncelli et al., 2014), leading to fluorescence enhancement in volumes much smaller than the ones dictated by the diffraction-limit of light.

FCS experiments on gold nanoparticles (AuNPs) demonstrated that the volume of observation can be drastically reduced below the diffraction limit thus increasing the detectable fluorophore concentration range (Estrada et al., 2008; Wang et al., 2011; Punj et al., 2013b; Punj et al., 2014; Flauraud et al., 2017; Winkler et al., 2017). These works showed that the presence of individual gold nanoparticles enables to reduce the detection volume by four orders of magnitude due to the gold nanoparticles' localized surface plasmon resonance. Also, by sensibly designing 2D antennas arrays it is possible to enhance the fluorescence of the few molecules diffusing in and out the antenna gap region (hot spot) while simultaneously deactivating the fluorescence background of the thousands of molecules diffusing within the diffraction limited volume (Flauraud et al., 2017). To simultaneously optimize field confinement, single-molecule detection and broadband operation, the geometrical parameters of the nano-sized antennas are typically first defined through numerical simulations. Plasmonic and dielectric nano-antennas with typical configurations including rods, dimers, bowties and trimers have already been used for this purpose (Dutta Choudhury et al., 2012; Kinkhabwala et al., 2012; Albella et al., 2013; Yuan et al., 2013; Caldarola et al., 2015; Khatua et al., 2015; Punj et al., 2015; Pradhan et al., 2016; Regmi et al., 2016).

Nano-apertures were also used to increase light-matter coupling (Wenger et al., 2007; Aouani et al., 2011). However, the combination of nano-antenna and aperture proves to be the best choice for this type of experiment since the antenna focuses the field while the aperture reduces background signal by preventing free molecules diffusing out of the gap from being excited (Punj et al., 2013a; Flauraud et al., 2017; Winkler et al., 2018). Figure 2B illustrates a schematic illustration of this type of antenna, along with simulations of field enhancement as a function of antenna gap distance. This antenna called "antenna-in-box" was used by Punj and colleagues to prove the detection and discrimination of different biomolecules at 10 μM concentration. They also studied the fluorescence enhancement and the changes in the detection volume for different nano-antenna gaps. In a later work, a full characterization and description of the fabrication method was presented (Flauraud et al., 2017). For instance, Figure 2C shows the fluorescence enhancement for different geometries of the "antenna-in-box" design as a function of the reduction in the detection volume compared to the typical confocal volume. This data illustrates that antennas with smaller gaps present the highest fluorescence enhancement, leading to the maximum reduction in the observation volume. Super-resolution microscopes nowadays can easily resolve distances of 40 nm, but often at the cost of a low temporal resolution which is not useful for some dynamics experiments in living systems. Therefore, the nano-focusing FCS technology appears to be a

powerful platform to investigate biological process with microsecond temporal resolution in sub-diffraction volumes.

Regarding the biology applications, Winkler and colleagues performed FCS on this antenna-in-box plasmonic platforms with different gap sizes to assess the dynamic nanoscale organization of mimetic biological membranes (Winkler et al., 2017). They studied the diffusion of a lipophilic fluorescent dye in the liquid-ordered (Lo) and liquid-disordered (Ld) phase of cholesterol in lipid membranes. Figure 2D shows the obtained normalized correlation curves for different antenna gaps which means different observation areas. The diffusion time for different observation areas is key to extract the diffusion environment of the molecules (i.e., free diffusion, nano-domains, meshwork). For example, free diffusion is characterized by a strict linear proportionality between the diffusion time and the observation area with a curve crossing the origin. Different slopes and interceptions with the time axis reveals different types of diffusion constrain as schematically shows in Figure 2D. In this work, a change in the diffusion law could be seen for different lipid compositions of the membrane. With this breadth of information, they found the presence of transient nanoscopic domains in both the Ld and Lo phases of ternary lipid mixtures with sizes in the range of 10 nm and short characteristic times around 30 μs for the Ld and 100 μs for the Lo phases [55]. These nano-antennas were also used to measure the influence of hyaluronic acid in the organization of mimetic lipid bilayers (Winkler et al., 2021). The study was complemented with atomic force microscopy and spectroscopy to assess the morphology and mechanical properties of the bilayers, resulting in changes of the micro and nano-organization with the presence or absence of the hyaluronic acid. Beyond mimetic systems, these platforms were also used to study the nanoscale dynamics of different lipids in living cells (Regmi et al., 2017).

Most recently, the "antenna-in-box" concept was also combined with multiplexed fluorescence readout using a sCMOS camera for simultaneous detection of 225 nano-antennas (Winkler et al., 2022). High-throughput arrayed detection of single-molecule dynamics at the nanoscale in living cell membranes was demonstrated. In addition, since field intensity relative to the aperture decay as a function of the axial distance, the axial positions of fluorophores was also determined in this work by utilizing the brightness-to-axial-distance relationship provided by antennas. Finally, in 2022, Barulin and colleagues introduce a new an optical horn antenna platform for single label-free proteins detection in the UV range via their natural ultraviolet fluorescence (Barulin et al., 2022). This antenna combines a conical horn reflector for fluorescence collection at ultrahigh angles with a metal nano-aperture for fluorescence enhancement and background screening. The horn antenna was used not only to achieve fluorescence enhancement but also enable UV

autofluorescence detection of single proteins above the background noise.

4 Discussion

Over the past two decades, several innovations in instrumentation and experimental techniques powered the resolution revolution in optical microscopy, including approaches based on single-molecule localization fluorescence microscopy (Lelek et al., 2021). Popularization of these fluorescence super-resolution techniques has begun to facilitate discoveries in different field of biology, by resolving protein organization with previously unattainable spatial detail. Whilst these techniques offer lateral resolution in the range of 10–40 nm, axial resolution is typically 2 to 4 times worse (Huang et al., 2008) and therefore different approaches over the years have been developed to achieve isotropic resolution in 3D (Bourg et al., 2015; Szalai et al., 2021; Velas et al., 2021). By levering the distance-dependent fluorescence lifetime modulation as response to the near-field coupling between fluorescent molecules and plasmon surface resonances in a thin metallic film, MIET currently offers a straightforward solution for isotropic 3D super-resolution imaging (Thiele et al., 2021). However, since its demonstration in 2014 (Chizhik et al., 2014), only three groups have applied MIET. Furthermore, the experimental realization of 3D super-resolution imaging via MIET either requires expensive cameras for wide-field FLIM imaging or a stable drift correction in the case of the confocal modality. In addition, it is rare for biological labs to have the expertise of fabricating the type of metal-coated slides required for MIET. Therefore, given the breadth of other recent approaches developed to achieve isotropic sub-30 nm resolution in 3D, the wider uptake of MIET in the biology community remains to be seen.

Like MIET, there is another technique, called graphene energy transfer (GIET), capable of decoding axial position from lifetime information using graphene as the "metal" layer. MIET uses the fluorescence signal coming from near-field electromagnetic coupling of a fluorophore's excited state to surface plasmons in planar metal films, whereas in graphene, the energy transfer from the excited fluorophore to electron-hole pairs resembles classical FRET between two molecular systems (Kaminska et al., 2019; Ghosh et al., 2021; Kamińska et al., 2021). In this case, the efficiency of this energy transfer process presents the advantage of increasing the distance dependent to around 25 nm, providing a dynamic range that lies between the operational range of FRET and MIET. As a result, GIET's localization accuracy improves by nearly an order of magnitude compared to MIET as there is a steeper distance-lifetime relationship (Ghosh et al., 2019). For example, in 2021, Raja and colleagues used this technology

to map the quasi-stationary states of the inner and outer mitochondrial membranes before and during ATP synthesis with ultra-high precision (i.e., sub-nanometer axial resolution) through fluorescence lifetime experiments (Raja et al., 2021). They showed that the mitochondrial intermembrane distance is (10.6 ± 0.6) nm in resting state, whereas it decreases to (8.6 ± 0.6) nm in the active state. In this sense, GIET provides a differential advantage to MIET in comparison to other approaches to decode axial information, as its level of axial accuracy is unrivalled opening the opportunity to resolve with ultra-high precision the conformational organization of proteins and complexes in their native environment. Among the new generation of ultra-resolved super-resolution imaging techniques, MINFLUX (Balzarotti et al., 2017), can achieve 1 nm lateral precision, offering a unique potential to be combined with MIET or GIET. p-MINFLUX (Masullo et al., 2020) is the best candidate for this combination as it provides direct access to fluorescence lifetime information, allowing a direct estimation of axial distances.

Besides spatial resolution, temporal resolution is also key to elucidate complex biological processes in living cells. The opportunities offered by plasmonic nano-antennas to confine the volumes of excitation/detection to the zepto-liter range provide a major step forward in fluorescence correlation spectroscopy techniques (Estrada et al., 2008). Whilst the first examples simply started with gold nanoparticles and nanorods, thanks to the rapid progress in numerical simulations and nanofabrication, high-performance antennas configurations could be developed and implemented in large scale to enhance the capabilities of FCS measurements. These configurations allowed to controllable confine excitation light to sizes between 10 and 50 nm with a temporal resolution in the order of the μs and enable single-molecule detection at concentrations range as high as 10 μM (Punj et al., 2013a; Winkler and García-Parajo, 2021). However, as the modulation of the fluorescence signal is usually dictated by the overlap between the molecular and the plasmon transition bands, the choice of fluorescent tags suitable for a specific antenna configuration might be restricted. Furthermore, this technique requires complex nanofabrication skills, and it is not trivial to engineer antennas design that have a broad band plasmon resonance. Ultimately, this limits the extension of these technologies to multi-color interrogation of distinct target proteins in living cells representing a key barrier to furthering our understanding of the vast and complex network of protein-protein interactions in the complex and crowed environment of living cells.

In conclusion, the combination of single-molecule imaging and spectroscopy with plasmonic has a lot to offer the life sciences since it can reveal unique information about the

distribution and dynamics of molecules in sub-diffraction dimensions.

Author contributions

CZ and SS wrote the manuscript and discussed the techniques to be introduced in the review article.

Funding

Conflict of interest

The authors declare that the research was conducted in the absence of any commercial or financial relationships that could be construed as a potential conflict of interest.

Publisher's note

All claims expressed in this article are solely those of the authors and do not necessarily represent those of their affiliated organizations, or those of the publisher, the editors and the reviewers. Any product that may be evaluated in this article, or claim that may be made by its manufacturer, is not guaranteed or endorsed by the publisher.

References

Albella, P., Poyli, M. A., Schmidt, M. K., Maier, S. A., Moreno, F., Sáenz, J. J., et al. (2013). Low-loss electric and magnetic field-enhanced spectroscopy with subwavelength silicon dimers. *J. Phys. Chem. C* 117 (26), 13573–13584. doi:10.1021/jp4027018

Anger, P., Bharadwaj, P., and Novotny, L. (2006). Enhancement and quenching of single-molecule fluorescence. *Phys. Rev. Lett.* 96 (11), 113002. doi:10.1103/physrevlett.96.113002

Aouani, H., Mahboub, O., Bonod, N., Devaux, E., Popov, E., Rigneault, H., et al. (2011). Bright unidirectional fluorescence emission of molecules in a nanoaperture with plasmonic corrugations. *Nano Lett.* 11 (2), 637–644. doi:10.1021/nl103738d

Balzarotti, F., Eilers, Y., Gwosch, K. C., Gynnå, A. H., Westphal, V., Stefani, F. D., et al. (2017). Nanometer resolution imaging and tracking of fluorescent molecules with minimal photon fluxes. *Science(1979)* 355 (6325), 606–612. doi:10.1126/science.aak9913

Barulin, A., Roy, P., Claude, J. B., and Wenger, J. (2022). Ultraviolet optical horn antennas for label-free detection of single proteins. *Nat. Commun.* 13 (1), 1842–1849. doi:10.1038/s41467-022-29546-4

Bauch, M., Toma, K., Toma, M., Zhang, Q., and Dostalek, J. (2014). Plasmon-enhanced fluorescence biosensors: A review. *Plasmonics* 9 (4), 781–799. doi:10.1007/s11468-013-9660-5

Berndt, M., Lorenz, M., Enderlein, J., and Diez, S. (2010). Axial nanometer distances measured by fluorescence lifetime imaging microscopy. *Nano Lett.* 10 (4), 1497–1500. doi:10.1021/nl100593x

Bezryadina, A., Zhao, J., Xia, Y., Zhang, X., and Liu, Z. (2018). High spatiotemporal resolution imaging with localized plasmonic structured illumination microscopy. *ACS Nano* 12 (8), 8248–8254. doi:10.1021/acsnano.8b03477

Bourg, N., Mayet, C., Dupuis, G., Barroca, T., Bon, P., Lécart, S., et al. (2015). Direct optical nanoscopy with axially localized detection. *Nat. Photonics* 9 (9), 587–593. doi:10.1038/nphoton.2015.132

Cade, N. I., Fruhwirth, G. O., Krasavin, A. V., Ng, T., and Richards, D. (2015). Fluorescence axial nanotomography with plasmonics. *Faraday Discuss.* 178, 371–381. doi:10.1039/c4fd00198b

Caldarola, M., Albella, P., Cortés, E., Rahmani, M., Roschuk, T., Grinblat, G., et al. (2015). Non-plasmonic nanoantennas for surface enhanced spectroscopies with ultra-low heat conversion. *Nat. Commun.* 6 (1), 7915–7918. doi:10.1038/ncomms8915

Chance, R. R., Prock, A., and Silbey, R. (1978). Molecular fluorescence and energy transfer near interfaces. *Adv. Chem. Phys.* 37, 1–65.

Chizhik, A. I., Chizhik, A. M., Khoptyar, D., Bär, S., Meixner, A. J., and Enderlein, J. (2011). Probing the radiative transition of single molecules with a tunable microresonator. *Nano Lett.* 11 (4), 1700–1703. doi:10.1021/nl200215v

Chizhik, A. I., and Enderlein, J. (2020). "Metal-induced energy transfer imaging," in *Nanoscale photonic imaging* (Cham: Springer), 227–239.

Chizhik, A. I., Gregor, I., and Enderlein, J. (2013). Quantum yield measurement in a multicolor chromophore solution using a nanocavity. *Nano Lett.* 13 (3), 1348–1351. doi:10.1021/nl400313z

Chizhik, A. I., Gregor, I., Schleifenbaum, F., Müller, C. B., Röling, C., Meixner, A. J., et al. (2012). Electrodynamic coupling of electric dipole emitters to a fluctuating mode density within a nanocavity. *Phys. Rev. Lett.* 108 (16), 163002. doi:10.1103/physrevlett.108.163002

Chizhik, A. I., Rother, J., Gregor, I., Janshoff, A., and Enderlein, J. (2014). Metal-induced energy transfer for live cell nanoscopy. *Nat. Photonics* 8 (2), 124–127. doi:10.1038/nphoton.2013.345

Chizhik, A. M., Ruhlandt, D., Pfaff, J., Karedla, N., Chizhik, A. I., Gregor, I., et al. (2017). Three-dimensional reconstruction of nuclear envelope architecture using dual-color metal-induced energy transfer imaging. *ACS Nano* 11 (12), 11839–11846. doi:10.1021/acsnano.7b04671

Chizhik, A. M., Wollnik, C., Ruhlandt, D., Karedla, N., Chizhik, A. I., Hauke, L., et al. (2018). Dual-color metal-induced and Förster resonance energy transfer for cell nanoscopy. *Mol. Biol. Cell* 29 (7), 846–851. doi:10.1091/mbc.e17-05-0314

Cortés, E., Huidobro, P. A., Sinclair, H. G., Guldbrand, S., Peveler, W. J., Davies, T., et al. (2016). Plasmonic nanoprobes for stimulated emission depletion nanoscopy. *ACS Nano* 10 (11), 10454–10461. doi:10.1021/acsnano.6b06361

Dutta Choudhury, S., Ray, K., and Lakowicz, J. R. (2012). Silver nanostructures for fluorescence correlation spectroscopy: Reduced volumes and increased signal intensities. *J. Phys. Chem. Lett.* 3 (19), 2915–2919. doi:10.1021/jz301229m

Enderlein, J. (1999). Single-molecule fluorescence near a metal layer. *Chem. Phys.* 247 (1), 1–9. doi:10.1016/s0301-0104(99)00097-x

Estrada, L. C., Aramendía, P. F., and Martínez, O. E. (2008). 10000 times volume reduction for fluorescence correlation spectroscopy using nano-antennas. *Opt. Express* 16 (25), 20597–20602. doi:10.1364/oe.16.020597

Flauraud, V., Regmi, R., Winkler, P. M., Alexander, D. T. L., Rigneault, H., van Hulst, N. F., et al. (2017). In-plane plasmonic antenna arrays with surface nanogaps for giant fluorescence enhancement. *Nano Lett.* 17 (3), 1703–1710. doi:10.1021/acs.nanolett.6b04978

Ford, G. W., and Weber, W. H. (1984). Electromagnetic interactions of molecules with metal surfaces. *Phys. Rep.* 113 (4), 195–287. doi:10.1016/0370-1573(84)90098-x

Ghosh, A., Chizhik, A. I., Karedla, N., and Enderlein, J. (2021). Graphene-and metal-induced energy transfer for single-molecule imaging and live-cell nanoscopy with (sub)-nanometer axial resolution. *Nat. Protoc.* 16 (7), 3695–3715. doi:10.1038/s41596-021-00558-6

Ghosh, A., Sharma, A., Chizhik, A. I., Isbaner, S., Ruhlandt, D., Tsukanov, R., et al. (2019). Graphene-based metal-induced energy transfer for sub-nanometre optical localization. *Nat. Photonics* 13 (12), 860–865. doi:10.1038/s41566-019-0510-7

Gottschalk, K. E., Port, F., Grandy, C., and Pfeil, J. (2022). "Super-resolution imaging with metal-induced energy transfer reveals effect of force on the actin cytoskeleton," in *Single molecule spectroscopy and superresolution imaging XV* (Washington, United States: SPIE), 79–82.

Grandy, C., Port, F., Pfeil, J., and Gottschalk, K. E. (2022). "Super-resolution imaging of the third dimension of the actin cytoskeleton using metal-induced energy transfer and micropatterning," in *Single molecule spectroscopy and superresolution imaging XV* (Washington, United States: SPIE), 64–71.

Gregor, I., Chizhik, A., Karedla, N., and Enderlein, J. (2019). Metal-induced energy transfer. *Nanophotonics* 8 (10), 1689–1699. doi:10.1515/nanoph-2019-0201

Huang, B., Wang, W., Bates, M., and Zhuang, X. (2008). Three-dimensional super-resolution imaging by stochastic optical reconstruction microscopy. *Sci. (1979)* 319 (5864), 810–813. doi:10.1126/science.1153529

Hwang, W., Seo, J., Kim, D., Lee, C. J., Choi, I. H., Yoo, K. H., et al. (2021). Large field-of-view nanometer-sectioning microscopy by using metal-induced energy transfer and biexponential lifetime analysis. *Commun. Biol.* 4 (1), 91–97. doi:10.1038/s42003-020-01628-3

Isbaner, S., Karedla, N., Kaminska, I., Ruhlandt, D., Raab, M., Bohlen, J., et al. (2018). Axial colocalization of single molecules with nanometer accuracy using metal-induced energy transfer. *Nano Lett.* 18 (4), 2616–2622. doi:10.1021/acs.nanolett.8b00425

Kaminska, I., Bohlen, J., Rocchetti, S., Selbach, F., Acuna, G. P., and Tinnefeld, P. (2019). Distance dependence of single-molecule energy transfer to graphene measured with DNA origami nanopositioners. *Nano Lett.* 19 (7), 4257–4262. doi:10.1021/acs.nanolett.9b00172

Kamińska, I., Bohlen, J., Yaadav, R., Schüler, P., Raab, M., Schröder, T., et al. (2021). Graphene energy transfer for single-molecule biophysics, biosensing, and super-resolution microscopy. *Adv. Mat.* 33 (24), 2101099. doi:10.1002/adma.202101099

Karedla, N., Chizhik, A. I., Gregor, I., Chizhik, A. M., Schulz, O., and Enderlein, J. (2014). Single-molecule metal-induced energy transfer (smMIET): Resolving nanometer distances at the single-molecule level. *ChemPhysChem* 15 (4), 705–711. doi:10.1002/cphc.201300760

Karedla, N., Chizhik, A. M., Stein, S. C., Ruhlandt, D., Gregor, I., Chizhik, A. I., et al. (2018). Three-dimensional single-molecule localization with nanometer accuracy using Metal-Induced Energy Transfer (MIET) imaging. *J. Chem. Phys.* 148 (20), 204201. doi:10.1063/1.5027074

Khatua, S., Yuan, H., and Orrit, M. (2015). Enhanced-fluorescence correlation spectroscopy at micro-molar dye concentration around a single gold nanorod. *Phys. Chem. Chem. Phys.* 17 (33), 21127–21132. doi:10.1039/c4cp03057e

Kinkhabwala, A. A., Yu, Z., Fan, S., and Moerner, W. E. (2012). Fluorescence correlation spectroscopy at high concentrations using gold bowtie nanoantennas. *Chem. Phys.* 406, 3–8. doi:10.1016/j.chemphys.2012.04.011

Krichevsky, O., and Bonnet, G. (2002). Fluorescence correlation spectroscopy: The technique and its applications. *Rep. Prog. Phys.* 65 (2), 251–297. doi:10.1088/0034-4885/65/2/203

Krichevsky, O., and Bonnet, G. (2002). Fluorescence correlation spectroscopy: The technique and its applications. *Rep. Prog. Phys.* 65 (2), 251–297. doi:10.1088/0034-4885/65/2/203

Krieger, J. W., Singh, A. P., Garbe, C. S., Wohland, T., and Langowski, J. (2014). Dual-color fluorescence cross-correlation spectroscopy on a single plane illumination microscope (SPIM-FCCS). *Opt. Express* 22 (3), 2358–2375. doi:10.1364/oe.22.002358

Lakowicz, J. R. (2006). *Principles of fluorescence spectroscopy*. Berlin, Germany: Springer.

Lelek, M., Gyparaki, M. T., Beliu, G., Schueder, F., Griffié, J., Manley, S., et al. (2021). Single-molecule localization microscopy. *Nat. Rev. Methods Prim.* 1 (1), 39–27. doi:10.1038/s43586-021-00038-x

Lukosz, W., and Kunz, R. E. (1977). Light emission by magnetic and electric dipoles close to a plane interface. I. Total radiated power. *J. Opt. Soc. Am.* 67 (12), 1607–1615. doi:10.1364/josa.67.001607

Magde, D., Elson, E., and Webb, W. W. (1972). Thermodynamic fluctuations in a reacting system—Measurement by fluorescence correlation spectroscopy. *Phys. Rev. Lett.* 29 (11), 705–708. doi:10.1103/physrevlett.29.705

Masullo, L. A., Steiner, F., Zähringer, J., Lopez, L. F., Bohlen, J., Richter, L., et al. (2020). Pulsed interleaved MINFLUX. *Nano Lett.* 21 (1), 840–846. doi:10.1021/acs.nanolett.0c04600

Masullo, L. A., Szalai, A. M., Lopez, L. F., and Stefani, F. D. (2021). Fluorescence nanoscopy at the sub-10 nm scale. *Biophys. Rev.* 13 (6), 1101–1112. doi:10.1007/s12551-021-00864-z

Oleksiievets, N., Mathew, C., Thiele, J. C., Gallea, J. I., Nevskyi, O., Gregor, I., et al. (2022)Single-molecule fluorescence lifetime imaging using wide-field and confocal-laser scanning microscopy: A comparative analysis. *Nano Lett.* [Internet]. doi:10.1021/acs.nanolett.2c01586

Oleksiievets, N., Sargsyan, Y., Thiele, J. C., Mougios, N., Sograte-Idrissi, S., Nevskyi, O., et al. (2022). Fluorescence lifetime DNA-PAINT for multiplexed super-resolution imaging of cells. *Commun. Biol.* 5 (1), 38–8. doi:10.1038/s42003-021-02976-4

Oleksiievets, N., Thiele, J. C., Weber, A., Gregor, I., Nevskyi, O., Isbaner, S., et al. (2020). Wide-field fluorescence lifetime imaging of single molecules. *J. Phys. Chem. A* 124 (17), 3494–3500. doi:10.1021/acs.jpca.0c01513

Olson, A. P., Ertsgaard, C. T., Elliott, S. N., and Lindquist, N. C. (2016). Super-resolution chemical imaging with plasmonic substrates. *ACS Photonics* 3 (3), 329–336. doi:10.1021/acsphotonics.5b00647

Port, F., Grandy, C., Pfeil, J., and Gottschalk, K. E. (2022). "Combining metal induced energy transfer and atomic force microscopy to probe the mechanoresponse of a focal adhesion," in *Single molecule spectroscopy and superresolution imaging XV* (Washington, United States: SPIE), 72–78.

Pradhan, B., Khatua, S., Gupta, A., Aartsma, T., Canters, G., and Orrit, M. (2016). Gold-nanorod-enhanced fluorescence correlation spectroscopy of fluorophores with high quantum yield in lipid bilayers. *J. Phys. Chem. C* 120 (45), 25996–26003. doi:10.1021/acs.jpcc.6b07875

Punj, D., de Torres, J., Rigneault, H., and Wenger, J. (2013). Gold nanoparticles for enhanced single molecule fluorescence analysis at micromolar concentration. *Opt. Express* 21 (22), 27338–27343. doi:10.1364/oe.21.027338

Punj, D., Mivelle, M., Moparthi, S. B., van Zanten, T. S., Rigneault, H., van Hulst, N. F., et al. (2013). A plasmonic 'antenna-in-box'platform for enhanced single-molecule analysis at micromolar concentrations. *Nat. Nanotechnol.* 8 (7), 512–516. doi:10.1038/nnano.2013.98

Punj, D., Regmi, R., Devilez, A., Plauchu, R., Moparthi, S. B., Stout, B., et al. (2015). Self-assembled nanoparticle dimer antennas for plasmonic-enhanced single-molecule fluorescence detection at micromolar concentrations. *ACS Photonics* 2 (8), 1099–1107. doi:10.1021/acsphotonics.5b00152

Punj, D., Rigneault, H., and Wenger, J. (2014). in *Single gold nanoparticles to enhance the detection of single fluorescent molecules at micromolar concentration using fluorescence correlation spectroscopy*. Editor V. Nanophotonics (Washington, United States: SPIE), 237–245.

Purcell, E. M., Torrey, H. C., and Pound, R. V. (1946). Resonance absorption by nuclear magnetic moments in a solid. *Phys. Rev.* 69 (1–2), 37–38. doi:10.1103/physrev.69.37

Raab, M., Schmied, J. J., Jusuk, I., Forthmann, C., and Tinnefeld, P. (2014). Fluorescence microscopy with 6 nm resolution on DNA origami. *ChemPhysChem* 15 (12), 2431–2435. doi:10.1002/cphc.201402179

Raja, S. O., Chizhik, A. I., Schmidt, C. F., Enderlein, J., and Ghosh, A. (2021). Mapping activity-dependent quasi-stationary states of mitochondrial membranes with graphene-induced energy transfer imaging. *Nano Lett.* 21 (19), 8244–8249. doi:10.1021/acs.nanolett.1c02672

Regmi, R., Berthelot, J., Winkler, P. M., Mivelle, M., Proust, J., Bedu, F., et al. (2016). All-dielectric silicon nanogap antennas to enhance the fluorescence of single molecules. *Nano Lett.* 16 (8), 5143–5151. doi:10.1021/acs.nanolett.6b02076

Regmi, R., Winkler, P. M., Flauraud, V., Borgman, K. J. E., Manzo, C., Brugger, J., et al. (2017). Planar optical nanoantennas resolve cholesterol-dependent nanoscale heterogeneities in the plasma membrane of living cells. *Nano Lett.* 17 (10), 6295–6302. doi:10.1021/acs.nanolett.7b02973

Simoncelli, S., Li, Y., Cortés, E., and Maier, S. A. (2018). Nanoscale control of molecular self-assembly induced by plasmonic hot-electron dynamics. *ACS Nano* 12 (3), 2184–2192. doi:10.1021/acsnano.7b08563

Simoncelli, S., Makarova, M., Wardley, W., and Owen, D. M. (2017). Toward an axial nanoscale ruler for fluorescence microscopy. *ACS Nano* 11 (12), 11762–11767. doi:10.1021/acsnano.7b07133

Simoncelli, S., Roberti, M. J., Araoz, B., Bossi, M. L., and Aramendia, P. F. (2014). Mapping the fluorescence performance of a photochromic–fluorescent system coupled with gold nanoparticles at the single-molecule–single-particle level. *J. Am. Chem. Soc.* 136 (19), 6878–6880. doi:10.1021/ja5025657

Simoncelli, S., Roller, E. M., Urban, P., Schreiber, R., Turberfield, A. J., Liedl, T., et al. (2016). Quantitative single-molecule surface-enhanced Raman scattering by optothermal tuning of DNA origami-assembled plasmonic nanoantennas. *ACS Nano* 10 (11), 9809–9815. doi:10.1021/acsnano.6b05276

Sultangaziyev, A., and Bukasov, R. (2020). Review: Applications of surface-enhanced fluorescence (SEF) spectroscopy in bio-detection and biosensing. *Sens. Biosensing. Res.* 30, 100382. doi:10.1016/j.sbsr.2020.100382

Szalai, A. M., Siarry, B., Lukin, J., Williamson, D. J., Unsain, N., Cáceres, A., et al. (2021). Three-dimensional total-internal reflection fluorescence nanoscopy with nanometric axial resolution by photometric localization of single molecules. *Nat. Commun.* 12 (1), 517. doi:10.1038/s41467-020-20863-0

Thiele, J. C., Helmerich, D. A., Oleksiievets, N., Tsukanov, R., Butkevich, E., Sauer, M., et al. (2020). Confocal fluorescence-lifetime single-molecule localization microscopy. *ACS Nano* 14 (10), 14190–14200. doi:10.1021/acsnano.0c07322

Thiele, J. C., Jungblut, M., Helmerich, D. A., Tsukanov, R., Chizhik, A., Chizhik, A. I., et al. (2021). Isotropic three-dimensional dual-color super-resolution microscopy with metal-induced energy transfer. *Sci. Adv.* 8 (23), eabo2506. doi:10.1126/sciadv.abo2506

Thiele, J. C., Jungblut, M., Helmerich, D. A., Tsukanov, R., Chizhik, A., Chizhik, A. I., et al. (2022). Isotropic three-dimensional dual-color super-resolution microscopy with metal-induced energy transfer. *Sci. Adv.* 8 (23), eabo2506. doi:10.1126/sciadv.abo2506

Vasilev, K., Stefani, F. D., Jacobsen, V., Knoll, W., and Kreiter, M. (2004). Reduced photobleaching of chromophores close to a metal surface. *J. Chem. Phys.* 120 (14), 6701–6704. doi:10.1063/1.1665719

Velas, L., Brameshuber, M., Huppa, J. B., Kurz, E., Dustin, M. L., Zelger, P., et al. (2021). Three-Dimensional single molecule localization microscopy reveals the topography of the immunological synapse at isotropic precision below 15 nm. *Nano Lett.* 21 (21), 9247–9255. doi:10.1021/acs.nanolett.1c03160

Wang, Q., Lu, G., Hou, L., Zhang, T., Luo, C., Yang, H., et al. (2011). Fluorescence correlation spectroscopy near individual gold nanoparticle. *Chem. Phys. Lett.* 503 (4–6), 256–261. doi:10.1016/j.cplett.2011.01.005

Wenger, J., Conchonaud, F., Dintinger, J., Wawrezinieck, L., Ebbesen, T. W., Rigneault, H., et al. (2007). Diffusion analysis within single nanometric apertures reveals the ultrafine cell membrane organization. *Biophysical J.* 92 (3), 913–919. doi:10.1529/biophysj.106.096586

Winkler, P. M., Campelo, F., Giannotti, M. I., and Garcia-Parajo, M. F. (2021). Impact of glycans on lipid membrane dynamics at the nanoscale unveiled by planar plasmonic nanogap antennas and atomic force spectroscopy. *J. Phys. Chem. Lett.* 12 (4), 1175–1181. doi:10.1021/acs.jpclett.0c03439

Winkler, P. M., and García-Parajo, M. F. (2021). Correlative nanophotonic approaches to enlighten the nanoscale dynamics of living cell membranes. *Biochem. Soc. Trans.* 49 (5), 2357–2369. doi:10.1042/BST20210457

Winkler, P. M., Regmi, R., Flauraud, V., Brugger, J., Rigneault, H., Wenger, J., et al. (2018). Optical antenna-based fluorescence correlation spectroscopy to probe the nanoscale dynamics of biological membranes. *J. Phys. Chem. Lett.* 9 (1), 110–119. doi:10.1021/acs.jpclett.7b02818

Winkler, P. M., Regmi, R., Flauraud, V., Brugger, J., Rigneault, H., Wenger, J., et al. (2017). Transient nanoscopic phase separation in biological lipid membranes resolved by planar plasmonic antennas. *Acs Nano* 11 (7), 7241–7250. doi:10.1021/acsnano.7b03177

Winkler, P. M., van Zanten, T. S., Mayor, S., and Garcia-Parajo, M. F. (2022). Multiplexed plasmonic nanoantennas for high throughput single molecule nanoscale dynamics in living cells. arXiv preprint arXiv:220112068.

Yuan, H., Khatua, S., Zijlstra, P., Yorulmaz, M., and Orrit, M. (2013). Thousand-fold enhancement of single-molecule fluorescence near a single gold nanorod. *Angew. Chem. Int. Ed. Engl.* 125 (4), 1217–1221. doi:10.1002/anie.201208125

Zelená, A., Isbaner, S., Ruhlandt, D., Chizhik, A., Cassini, C., Klymchenko, A. S., et al. (2020). Time-resolved MIET measurements of blood platelet spreading and adhesion. *Nanoscale* 12 (41), 21306–21315. doi:10.1039/d0nr05611a